Integration
geoscience
engineering
partnership
geoConvention 2013

Seismic behaviour of CO_2 saturated Fontainebleau sandstone under in situ conditions

Md Mizanul Huq Chowdhury*, University of Alberta, Edmonton, AB, Canada,
mhchowdh@ualberta.ca
and
Douglas R. Schmitt, University of Alberta, Edmonton, AB, Canada,
dschmitt@ualberta.ca

Summary

Understanding the seismic response of a rock in the CO_2 sequestration is important for the societal acceptance of geological greenhouse gas sequestration and for monitoring of volcanic hazards. Additionally, the study of the effect of CO_2 on seismic wave propagation is scientifically interesting because CO_2 can exist in gas, liquid, and supercritical fluid phases over the modest temperature and pressure ranges typically accessible in the upper 2 km of the earth's crust, CO_2's critical point lies near 31˚C and 7.4 MPa. We have carried out a series of ultrasonic pulse transmission experiments on several samples of fully CO_2 saturated Fontainebleau sandstone over pore fluid pressure ranges of 1 MPa to 20 MPa and at two constant temperatures below (21˚C) and above (50˚C) the critical temperature, these ranges were chosen to cross the gas-liquid and gas-supercritical transitions, respectively.

Introduction

In a geological CO_2 sequestration project CO_2 leakage is a vital concern for which monitoring and verifying the subsurface movement and phase behavior of the injected CO_2 is important to ensure the storage integrity. Seismic methods are seemed to be a convenient way to monitor the changes in subsurface in a CO_2 sequestration as seismic velocities are equally sensitive to a rock's mineralogical composition, porosity and pore fluid contents. However, proper interpretation of such field observations requires appropriate knowledge of the material's seismic properties. Here we report on the simultaneous measurement of ultrasonic compressional and shears wave velocities through saturated Fontainebleau sandstones. Fontainebleau sandstone is collected from the Paris region, France. It shows a large porosity variation from 2%-28% and consists of pure quartz (99.8%). Its pore geometry shows significant variation with porosity and has a wide spectrum of microstructure. The main motivation of this work is to obtain an understanding on the rock physics involved with CO_2 as pore fluid.

Physical and elastic properties of CO_2

The bulk modulus and density phase diagrams of CO_2 are shown in the Fig. 1 as function of pressure and temperature on the basis of Span and Wagner's (1996) thermodynamic model. The critical point of CO_2 according to this model is at 31^0 C and at 7.4 MPa. Depending on the subsurface situations CO_2 can be either gas or liquid under this temperature and pressure. A sudden change in physical properties of CO_2 clearly indicates the gas-liquid boundary in the diagram, which gradually vanishes as

the red point (critical point) reached. The supercritical fluid phase state starts just after that point. The supercritical fluid phase has distinct property-it shows the physical behavior of gas and liquid in the same time. This results a smooth transition of liquid-supercritical or gas-supercritical phases.

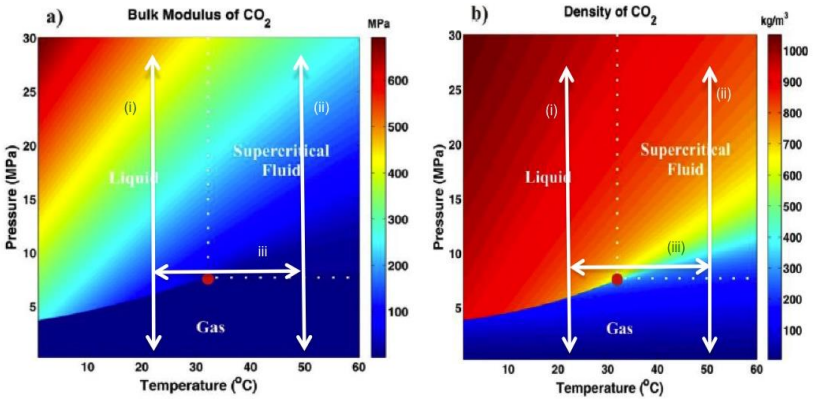

Fig 1: CO_2 phase diagrams as function of pressure and temperature according to the thermodynamic model of Span and Wagner (1996). Fig 1(a) gives the bulk modulus and the fig 1(b) is for density phase diagram of CO_2 .The critical point of CO_2 is clearly indicated by the red dot in both phase diagrams. The gas-liquid boundary is easily noticeable because of the sudden change in physical properties. The white dotted line gives the boundaries for the supercritical fluid phase. White arrows shows three cases of our measurements as (i) gaseous to liquid, (ii) gaseous to supercritical fluid and (iii) liquid to supercritical fluid transitions.

Gassmann's Rock-fluid interaction Model:

Gassmann's equation is one of the simple and widely used rock-fluid interaction models applicable for seismic frequency region ~ 100 Hz. He considered the elementary elasticity of the pore fluid and mineral grains of the sample that is saturated.
He also considered some assumptions to formulate his equation that are:
1) A microscopically homogenous and isotropic medium,
2) Similar bulk and shear moduli for all minerals that constitute the rock sample,
3) A zero fluid viscosity and a free movement of the fluids in pore regions which are interconnected,
4) Completely saturated pore space all times,
5) No interaction between pore fluid and rock minerals i.e. no change in rock's stiffness,
6) Quasi-static conditions are maintained to have frequencies low enough.
In this Gassmann's formulation the medium's saturated bulk modulus, K_{sat}, has relation with frame modulus, K_{dry}, bulk modulus of the mineral grains, K_s, bulk modulus of the fluid, K_f, and the porosity of the rock medium, ϕ , through the following:

$$K_{sat} = K_{dry} + \frac{(1-\frac{K_{dry}}{K_s})^2}{\frac{\phi}{K_f} + \frac{1-\phi}{K_s} + \frac{K_{dry}}{K_s^2}} \quad , \ \mu_{sat} = \mu_{dry} \tag{1.1}$$

Here μ_{sat} & μ_{dry} are the saturated and dry shear modulus of the rock frame. P- and S-wave velocities than can be calculated using the following formulas:

$$V_p = \sqrt{\frac{K_{sat} + \frac{4}{3}\mu_{sat}}{\rho_{sat}}} \ , \quad V_s = \sqrt{\frac{\mu_{sat}}{\rho_{sat}}} \ , \quad \rho_{sat} = (1-\phi)\rho_s + \phi\rho_f \ . \tag{1.2}$$

Here ρ_{sat} is the saturated density and ρ_f is the fluid density.

Sample Properties

At this writing, two Fontainebleau samples have been used in our measurements. The table summarized their properties and the Fig 2 shows the samples:

Properties	Fontainebleau 1	Fontainebleau 2
Mass (gm)	117.1	167.2
Bulk Volume (cm^3)	45.16	65.59
Grain Density (kg/m^3)	2650	2650
Bulk Density (kg/m^3)	2593	2549.16
Porosity (%)	10	12.5
Modal Pore size (μm)	20	20

Fig 2: Fontainebleau samples.

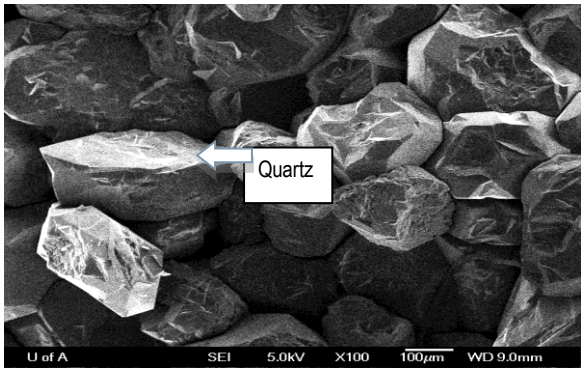

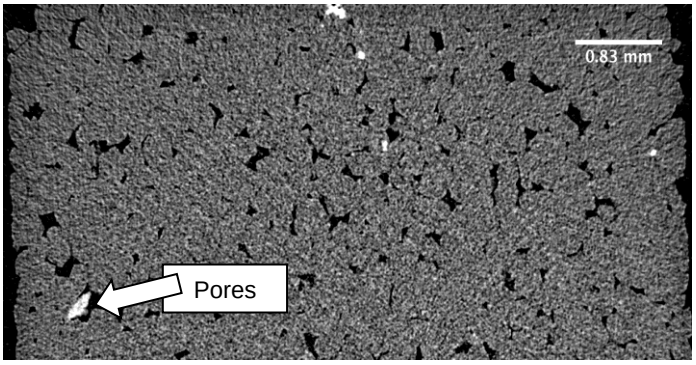

Fig 3: left panel: SEM image. Right panel: micro CT image of the Fontainebleau sample.

Experimental setup & protocol

The ultrasonic pulse transmission method was used to determine P- and S-wave velocities. This method conceptually involves measuring the travel time of the ultrasonic wave travelling through the sample. The experimental set up consists of several functional units such as pulse generator, source/receiving transducers, a digital oscilloscope, a pressure vessel that can apply confining pressure up to 200 MPa, a fluid reservoir, and a thermocouple.

Fig 4 shows simplified schematic set-up of the experiment.

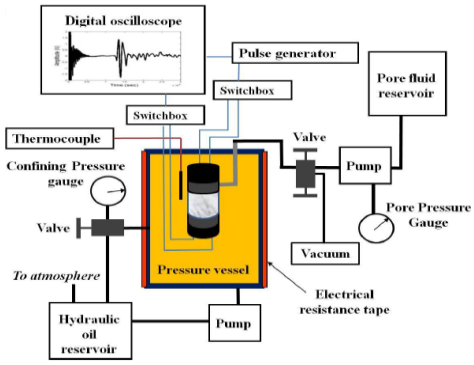

Fig 4: Schematic diagram of the set-up.

A series of measurements are done in our experiment including dry runs where the sample is free from any liquid or gas to obtain the dry frame moduli, Nitrogen runs to test the effective pressure, than various CO_2 saturated runs and at the end H_2O runs. The whole experimental protocol is shown in the following flow chart:

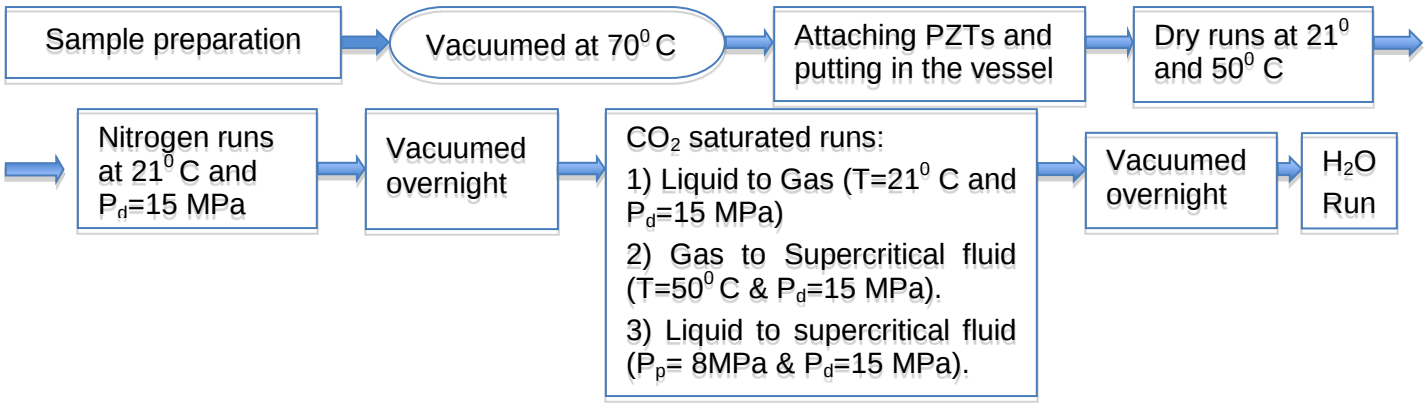

In the flow chart PZT stands for Piezoelectric Transducer, P_d for differential pressure and P_p for pore pressure.

Examples:

Dry runs: In these measurements the sample is free from any fluid. We did two dry run measurements one in 21^0 C and another one with 50^0 C. Fig 4 shows the P-and S-wave velocity vs time plots of the dry measurements.

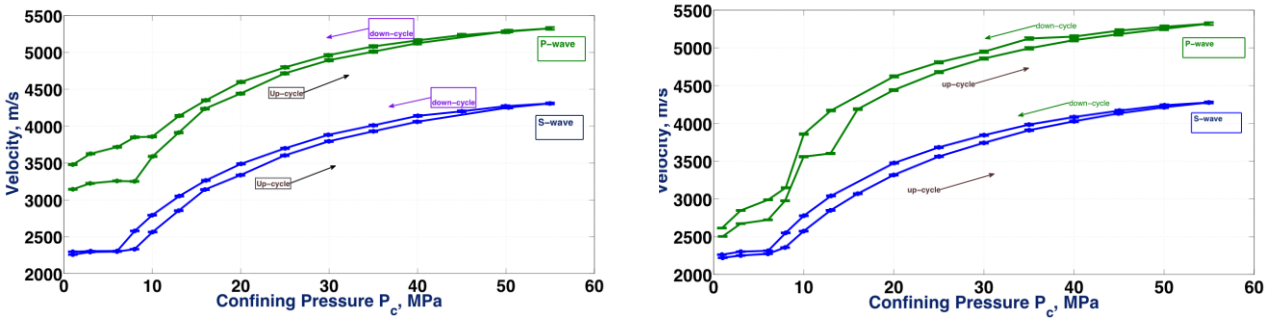

Fig 4. Dry measurements for 21^0 C (left) and 50^0 C (right). As confining pressure increases the wave velocities also increases. At a given confining pressure the wave velocities during up-cycle (pressurizing) is always lower than down-cycle (depressurizing) showing wave velocity hysteresis. The wave velocities increase rapidly at lower pressure but this increment diminishes at higher pressure because of number of closure of compliant pores reduces at high pressure.

Nitrogen runs: After the dry runs, the Nitrogen runs are done to check the effective pressure. In these measurements we noted a very less variations in velocities but still we saw some hysteresis in the data Fig 5 shows the nitrogen run measurements.

Fig 5. Nitrogen runs- left one is for P-wave velocity and the right one shows the S-wave velocity plot.

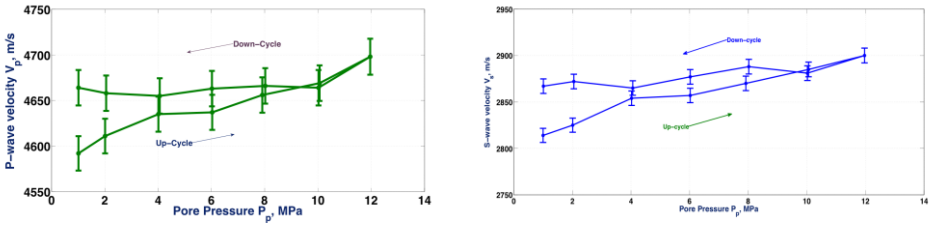

CO_2 runs: Three different CO_2 saturated runs were done to see the transition of 1) liquid to gas, 2) gas to supercritical fluid and 3) liquid to supercritical fluid. Fig 6, 7 and 8 shows the three transitions respectively:

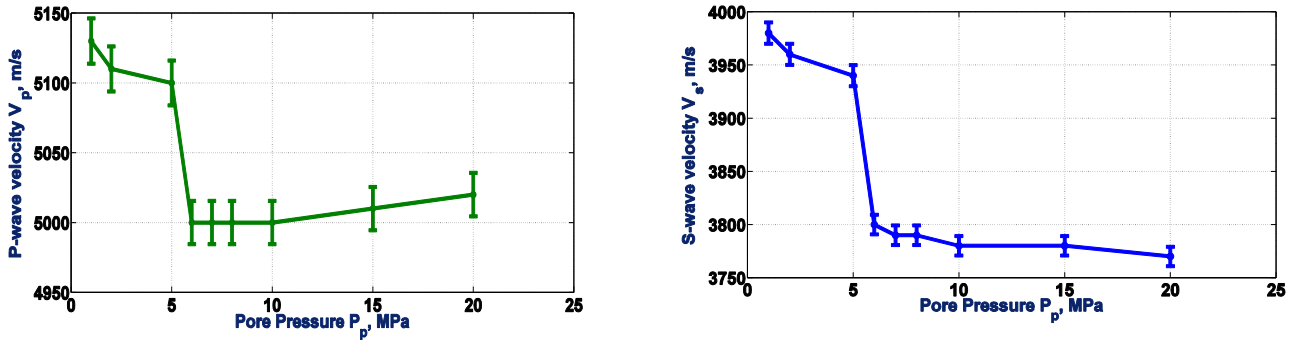

Fig 6: Liquid to Gas transition measurements. For P-wave (left) we see a clear 1.96% velocity drop around their vapour pressure (P_p=5-6 MPa) when the transition happens while for S-wave (right) we see a significant velocity drop of ~3% on that pressure range. In the both cases the temperature was constant (T~ 21^0 C).

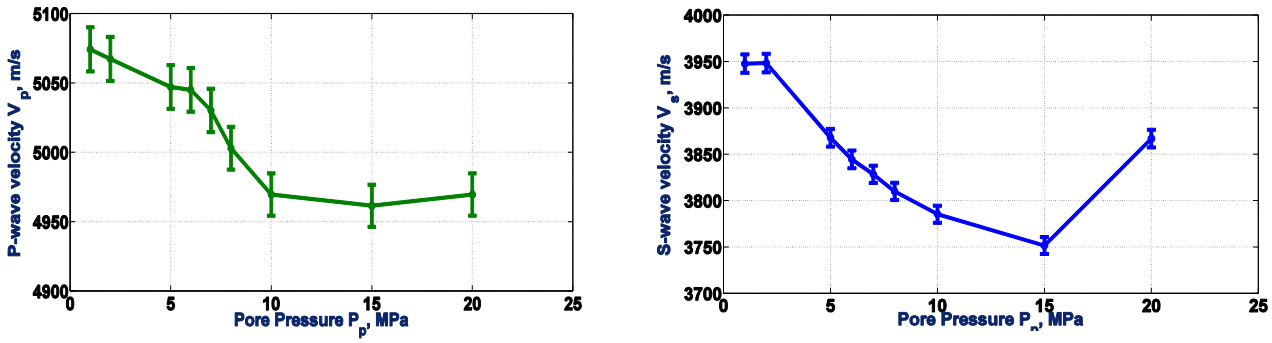

Fig 7: Gas to supercritical transition measurement. Both P-wave (left) and S-wave (right) velocities show a gradual change near transition pressure (P_p ~7—8 MPa).

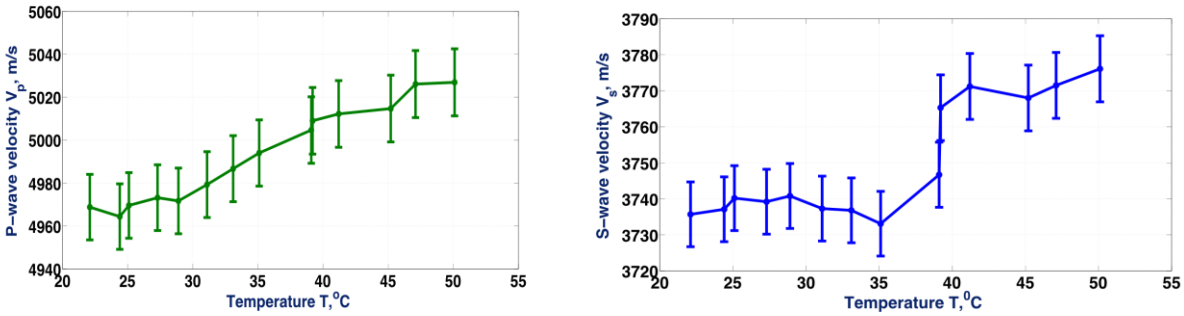

Fig 8: Liquid to supercritical fluid transition measurements. The transition is gradual around the transition temperature ~31^0 C for both P-wave (left) and S-wave (right) case.

Comparison between observation and Gassmann's model prediction: Gassmann's equation is used to predict the P- and S-wave velocities in the same range of temperatures and pressures and Fig. 9 shows the comparison for all three cases. We can see that the trend for each case is similar but there is a difference in the

velocities. Gassmann's equations are applicable for low frequency (~100 Hz) measurement but we did our runs at high frequency (~1 MHz) and all the assumptions of the model cannot be fulfill for a real measurements.

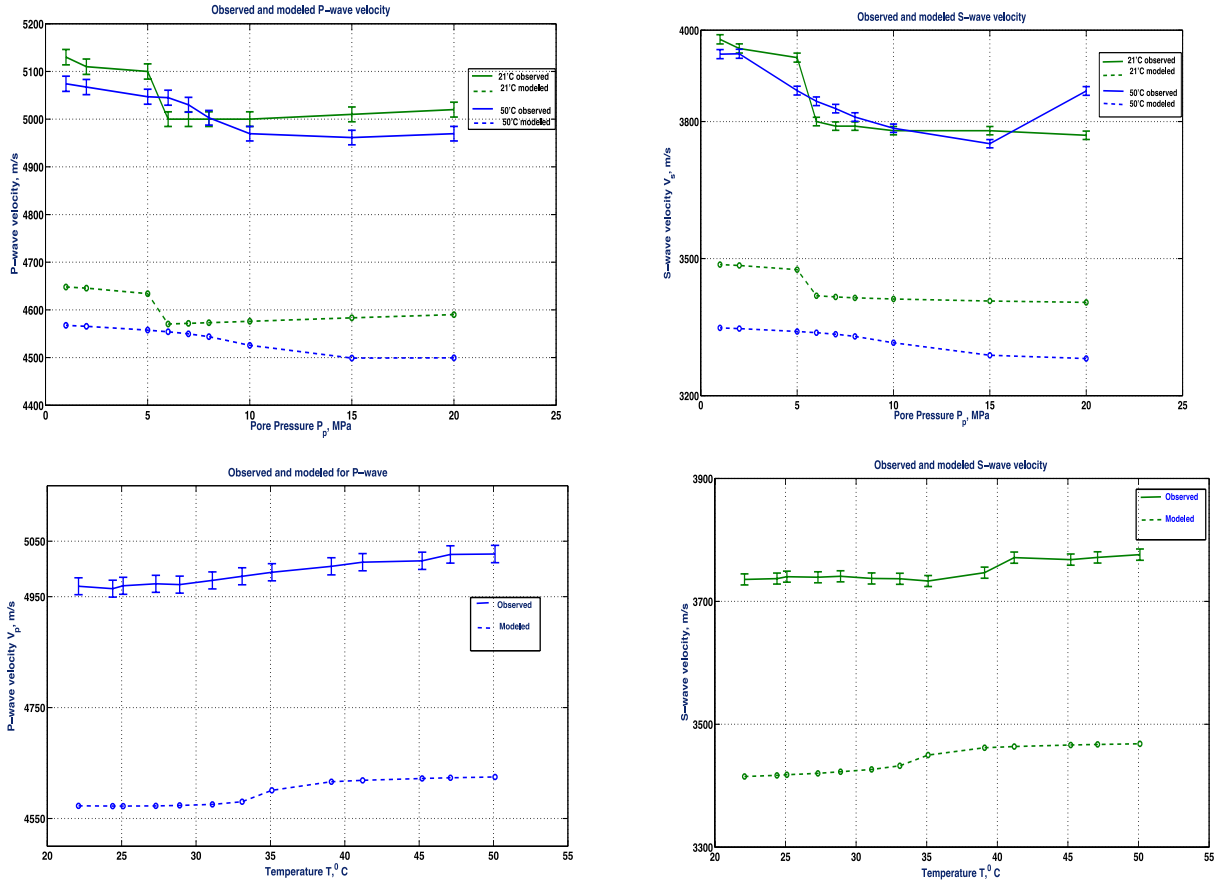

Fig. 9 : Comparison of the observed and the Gassmann's model prediction for all three cases of CO_2 saturated runs.

Conclusions

We have measured P- and S-wave velocities for various pressure and temperature conditions in two Fontainebleau sandstones to check the change in velocities during the phase transition. The velocities change gradually across the gas-supercritical and liquid supercritical transitions in agreement with the nature of these second order phase transitions. The gas-liquid transition is, conversely, a first order transition discontinuous in CO_2 density and bulk modulus and explains the abrupt changes in a wave speeds across the phase boundary. However in the real situation the rock may not only saturated with CO_2 , there may be other pore fluid present there too to consider. The comparison between the observed data and Gassmann's model predictions are also shown where we see a similar trend for the all three cases for CO_2 saturation measurements.

Acknowledgements

Md Mizanul Huq Chowdhury would like to thank professor Schmitt group's research professional Randy Kofman and the postdoctoral fellow Gautier Njiekak for their technical support in making this experiment.

References

Yam, Helen, CO_2 rock physics: a laboratory study, 2011,MSc thesis, Department of Physics, University of Alberta.

Span, R., and Wagner, W., 1996, A new equation of state for carbon dioxide covering the fluid region from triple-point temperature to 1100K at pressure up to 800 MPa, J. Phys. Chem. Ref. Data, 25, 1509-1596.

Gassmann, F., 1951,Uber die elastizitat poroser medien:Vierteljahrsschrift der Naturforschenden Gesellschaft in Zurich, 96, 1–23.